



# Infrared and Near-Infrared Spectrometry of Anatase and Rutile Particles Bandgap Excited in Liquid

Fu, Zhebin

Onishi, Hiroshi

---

**(Citation)**

The Journal of Physical Chemistry B, 127(1):321-327

**(Issue Date)**

2023-01-12

**(Resource Type)**

journal article

**(Version)**

Version of Record

**(Rights)**

© 2022 The Authors. Published by American Chemical Society.

This article is licensed under the Creative Commons Attribution-NonCommercial-NoDerivatives 4.0 International license.

**(URL)**

<https://hdl.handle.net/20.500.14094/0100485945>



# Infrared and Near-Infrared Spectrometry of Anatase and Rutile Particles Bandgap Excited in Liquid

Published as part of *The Journal of Physical Chemistry virtual special issue "Hiro-o Hamaguchi Festschrift"*.

Zhebin Fu\* and Hiroshi Onishi\*



Cite This: *J. Phys. Chem. B* 2023, 127, 321–327



Read Online

ACCESS |



Metrics & More

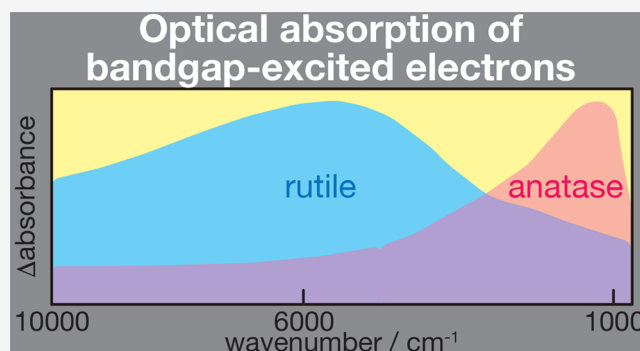


Article Recommendations



Supporting Information

**ABSTRACT:** Chemical conversion of materials is completed in milliseconds or seconds by assembling atoms over semiconductor photocatalysts. Bandgap-excited electrons and holes reactive on this time scale are key to efficient atom assembly to yield the desired products. In this study, attenuated total reflection of infrared and near-infrared light was applied to characterize and quantify the electronic absorption of  $\text{TiO}_2$  photocatalysts excited in liquid. Nanoparticles of rutile or anatase were placed on a diamond prism, covered with liquid, and irradiated by steady UV light through the prism. Electrons excited in rutile particles (JRC-TIO-6) formed small polarons characterized by a symmetric absorption band spread over  $10000\text{--}700\text{ cm}^{-1}$  with a maximum at  $6000\text{ cm}^{-1}$ . Electrons in anatase particles (JRC-TIO-7) created large polarons and produced an asymmetric absorption band that gradually strengthened at wavenumbers below  $5000\text{ cm}^{-1}$  and sharply weakened at  $1000\text{ cm}^{-1}$ . The absorption spectrum of large electron polarons in TIO-7 was compared with the absorption reported in a Sr-doped  $\text{NaTaO}_3$  photocatalyst, and it was suggested that excited electrons were accommodated as large polarons in  $\text{NaTaO}_3$  photocatalysts efficient for artificial photosynthesis. UV-light power dependence of the absorption bands was observed in  $\text{N}_2$ -exposed decane liquid to deduce electron–hole recombination kinetics. With light power density  $P > 200\text{ W m}^{-2}$  (TIO-6) and  $2000\text{ W m}^{-2}$  (TIO-7), the polaron absorptions were enhanced with absorbance being proportional to  $P^{1/2}$ . The observed  $1/2$ -order power law suggested recombination of multiple electrons and holes randomly moving in each particle. Upon excitation with smaller  $P$ , the power-law order increased to unity. The unity-order power law was interpreted with recombination of an electron and a hole that were excited by the same photon. In addition, an average lifetime of 1 ms was estimated with electron polarons in TIO-6 when weakly excited at  $P = 20\text{ W m}^{-2}$  to simulate solar-light irradiation.



## 1. INTRODUCTION

Chemical conversion over semiconductor photocatalysts has been extensively investigated but not yet understood completely. Transient absorption spectroscopy (TAS) determines the initial fate of the electrons and holes excited in photocatalysts. Photon absorption and electronic excitation are followed by exciton formation or separation and subsequent charge carrier transport from the bulk to the surface.<sup>1–3</sup> The electron-based steps are initiated in femtoseconds and completed in microseconds, whereas reaction products are formed in milliseconds or even seconds via the assembly of atoms on the surface.<sup>4,5</sup> TAS with short light pulses for photocatalyst excitation is not always suitable for characterizing excited charge carriers reactive on the time scale of atom assembly. Short-life charge carriers detected in TAS may or may not contribute atom assembly in their limited lifetimes.

In this study, Fourier transform (FT) spectroscopy in a wavenumber range of  $10000\text{--}700\text{ cm}^{-1}$  is applied to characterize and quantify electrons excited in two  $\text{TiO}_2$  polymorphs,

namely, rutile and anatase, irradiated with steady ultraviolet (UV) light. Excited electrons absorb infrared (IR), near-IR, or visible light according to the host semiconductors in which they are created. A number of earlier studies<sup>6–12</sup> reported that electronic absorption appeared in the IR and near-IR regions when  $\text{TiO}_2$  photocatalysts are excited in vacuum and vapor environments.

The other requirement in this study is operando characterization. Because most photocatalysts are operated in liquid environments, our spectrometry should be conducted in liquid. This is a difficult task because IR light used for probing is

**Received:** October 22, 2022

**Revised:** December 2, 2022

**Published:** December 21, 2022



absorbed by the liquid, while UV light for excitation is absorbed by photocatalyst particles. The ordinary setup for attenuated total reflection (ATR) through a prism made of ZnSe, Si, etc. is convenient to guide probing light into photocatalyst particles in liquid but problematic for delivering light for excitation.

## 2. METHODS AND MATERIALS

This study used an ATR assembly with a diamond prism (Figure 1) constructed by Jasco in our earlier study.<sup>13</sup> The angle of

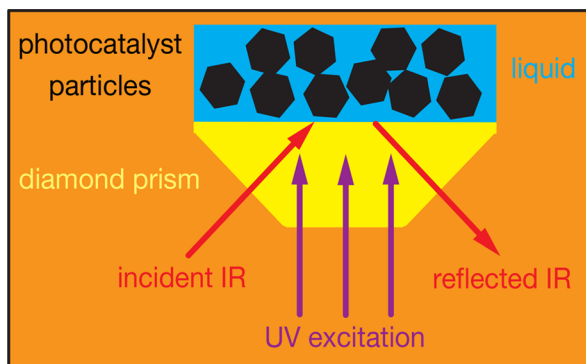


**Figure 1.** A prism assembly for ATR spectroscopy under UV light irradiation through the prism. An isosceles trapezoidal prism with a circular reflection plane of 1.8 mm in diameter is assembled with an LED or Hg–Xe lamp as the UV light source.

probe-light incidence was fixed at  $45^\circ$  from the normal of the reflection plane. The depths of IR (wavenumber:  $1000\text{ cm}^{-1}$ ) and near-IR (wavenumber:  $10000\text{ cm}^{-1}$ ) light penetration into water were estimated to be 1.5 and  $0.15\text{ }\mu\text{m}$  with the refractive indexes of diamond and water, 2.38 and 1.32, respectively.<sup>14</sup> The refractive index of  $\text{TiO}_2$  particles mixed with water should be greater than that of water to accordingly increase penetration depth. A light-emitting diode (LED; 365 nm center wavelength, M365L3, Thorlabs) provided UV light for bandgap excitation through the prism to the volume probed by IR light. The UV light power density on the reflection plane was calibrated using a photodiode sensor (PD-300, Ophir) and tuned in a range of  $20\text{--}3600\text{ W m}^{-2}$ . A Hg–Xe lamp (200 W, UVF-204S, San-Ei Electric) was used instead of the LED when intense UV light ( $9.0\text{ kW m}^{-2}$  on the reflection plane) was necessary.

The prism assembly was set in a Fourier transform infrared spectrometer (FT/IR-6600, Jasco). The reflection plane was irradiated with He–Ne laser light (wavelength: 633 nm) for interferometer calibration, which was unable to excite  $\text{TiO}_2$  particles across the bandgap. To measure IR absorption at  $7000\text{--}700\text{ cm}^{-1}$ , a ceramic light source was used with a mercury–cadmium–telluride (MCT) detector, while a halogen lamp and an InGaAs detector were employed in near-IR spectrometry at  $10000\text{--}4000\text{ cm}^{-1}$ . The acquisition time was 19 s per IR spectrum and 52 s per near-IR spectrum with a wavenumber resolution of  $8\text{ cm}^{-1}$ . Figure S1 shows the near-IR transmittance spectrum of the prism assembly with a water droplet on the reflection plane. A corresponding spectrum in the IR region is available in the Supporting Information of ref 13. IR transmittance decreased to  $<30\%$  at  $2500\text{--}1800\text{ cm}^{-1}$  because of the absorption in the diamond prism. Hence, absorbance spectra of photocatalysts are shown herein in the wavenumber ranges of  $10000\text{--}2500$  and  $1800\text{--}700\text{ cm}^{-1}$ . The absorbance change induced by UV light was observed and quantified in an absorbance range of  $10^{-1}\text{--}10^{-3}$ .

$\text{TiO}_2$  photocatalyst particles were placed on the reflection plane of the prism and covered with a liquid droplet. The prism assembly inside the spectrometer was exposed to air or  $\text{N}_2$  gas to make the droplet anaerobic when necessary. Figure S2 shows the near-IR absorbance spectra of water and other liquids observed on the prism assembly. Two  $\text{TiO}_2$  photocatalysts provided by the Catalysis Society of Japan were used: rutile  $\text{TiO}_2$  (JRC-TIO-6) and anatase  $\text{TiO}_2$  (JRC-TIO-7). The nominal particle sizes of TIO-6 and TIO-7 were 15 and 8 nm, respectively. X-ray diffraction patterns of the photocatalysts are shown in Figure S3. The size of particles was much less than the penetration depth of probe light. Hence, probe-light absorption averaged over multiple particles was observed. The Supporting Information lists the reagents used in preparing liquid droplets.

## 3. RESULTS

**3.1. Absorbance Change Induced by UV Light Irradiation.** Absorbance change ( $\Delta\text{absorbance}$ ) was deduced from the absorbance spectra recorded in the presence and absence of UV light irradiation. We present in Figure 2 the

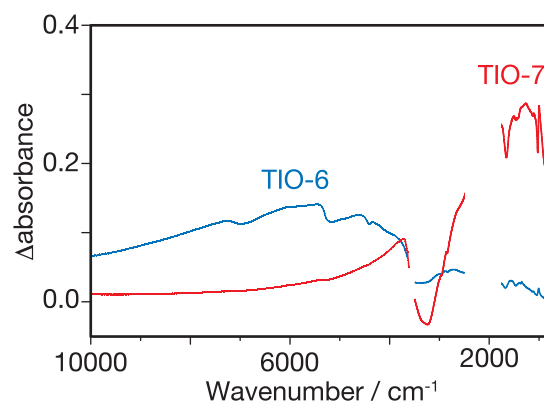


**Figure 2.** Absorbance change ( $\Delta\text{absorbance}$ ) spectra of  $\text{TiO}_2$  particles. TIO-6 (blue spectrum) and TIO-7 (red spectrum) were irradiated in a methanol–water mixture (50 vol %) exposed to  $\text{N}_2$ . UV light source: Hg–Xe lamp. UV light power density on the reflection plane of the prism:  $9.0\text{ kW m}^{-2}$ . Probe light source and detector for  $10000\text{--}3800\text{ cm}^{-1}$ : halogen lamp and InGaAs detector. Probe light source and detector for  $3800\text{--}700\text{ cm}^{-1}$ : ceramic source and MCT detector. The spectra are shown in the wavenumber ranges of  $10000\text{--}2500$  and  $1800\text{--}700\text{ cm}^{-1}$  because IR transmittance through the prism decreased to  $<30\%$  at  $2500\text{--}1800\text{ cm}^{-1}$ .

$\Delta\text{absorbance}$  spectra of TIO-6 and TIO-7 in a methanol–water mixture (50 vol %) induced by intense irradiation ( $9.0\text{ kW m}^{-2}$ ) with the Hg–Xe lamp because  $\Delta\text{absorbance}$  of the two photocatalysts was not detectable in pure water. Methanol is a hole-scavenging reagent that increases the population of electrons that are excited and not yet recombined with holes, as demonstrated in a number of  $\text{TiO}_2$  photocatalysts exposed to its vapor.<sup>15</sup>

On TIO-6 of rutile, a symmetric absorption band appeared in the full wavenumber window of  $10000\text{--}700\text{ cm}^{-1}$  with a maximum at  $6000\text{ cm}^{-1}$ . A narrower, asymmetric absorption band was recognized on TIO-7 of anatase;  $\Delta\text{absorbance}$  gradually increased at wavenumbers below  $5000\text{ cm}^{-1}$ , making a peak at  $1300\text{ cm}^{-1}$  and rapidly decreasing at  $1000\text{ cm}^{-1}$ . The two  $\Delta\text{absorbance}$  bands were present in the methanol–water mixture whereas they were absent in pure water. This set of results allowed us to assign the two  $\Delta\text{absorbance}$  bands to

electrons excited in the  $\text{TiO}_2$  photocatalysts. Photoexcited holes were rapidly consumed in methanol oxidation. Excited electrons complementary to the holes left in photocatalyst particles and slowly consumed in water reduction to produce  $\text{H}_2$ . In a steady state, a small number of holes and a large number of electrons are present in a particle. Hence, the particle should have been positively charged and neutralized with the anion atmosphere in the solution.

Negative  $\Delta$ absorbance peaks superimposed at  $3700\text{--}3000$  and  $1600\text{ cm}^{-1}$  on the spectra of TIO-6 and TIO-7 correspond to the vibrational absorption of water bleached by UV light irradiation. Bleached overtones of water vibration appeared at  $7000$  and  $5200\text{ cm}^{-1}$  on the spectrum of TIO-6.

UV-light-induced  $\Delta$ absorbance was further examined in the solutions of electron scavenging reagents  $\text{FeCl}_3$  ( $50\text{ mmol L}^{-1}$ )<sup>16</sup> and  $\text{NaIO}_3$  ( $50\text{ mmol L}^{-1}$ ).<sup>17</sup> As shown in Figure S4, absorbance change was not detectable; this supports our assignment of the bands present in Figure 2 to excited electrons. It is also suggested that holes in the  $\text{TiO}_2$  particles presented optical absorption, if any, out of the wavenumber range examined in this study. Hole population should have been enhanced in the electron scavengers, but no additional band appeared in  $\Delta$ absorbance.

The symmetric spectrum on TIO-6 and the asymmetric spectrum on TIO-7 suggested qualitatively different properties of the electrons excited in the two  $\text{TiO}_2$  photocatalysts. The symmetric and asymmetric spectra are consistent with those reported in a transient absorption study by Yamakata et al.<sup>11</sup> They observed UV-light-induced transient  $\Delta$ absorbance with rutile and anatase particles placed in a vacuum or vapor environment. Two different anatase particles (one  $21\text{ nm}$  in diameter and the other  $15\text{ nm}$  in diameter) presented a  $\Delta$ absorbance band that monotonously strengthened at wavenumbers of  $4000$  to  $1000\text{ cm}^{-1}$  in Figure 1 of ref 11. Rutile particles having diameters of  $40$  and  $15\text{ nm}$  exhibited two bands that peaked at  $22000$  and  $13000\text{ cm}^{-1}$  with a slight increment centered at  $6000\text{ cm}^{-1}$  in Figure 3 of ref 11. They assigned the absorption increment at  $6000\text{ cm}^{-1}$  to excited electrons according to the increment enhanced in the presence of methanol vapor. Shinoda and Murakami<sup>12</sup> also reported a  $\Delta$ absorbance band at  $3000\text{--}1000\text{ cm}^{-1}$  for anatase particles exposed to ethanol vapor, while rutile particles presented a broad band centered at  $8000\text{--}7000\text{ cm}^{-1}$ . Savory and McQuillan<sup>18</sup> reported an absorbance change that peaked at  $880\text{ cm}^{-1}$  for anatase particles  $23\text{ nm}$  in diameter excited under water. Our findings in the methanol–water mixture are consistent with their reports in vacuum/vapor/water environments. The symmetric and asymmetric bands are intrinsic with electrons excited in rutile and anatase regardless of environments to suggest excited electrons accommodated in bulk particles.

This is in contrast to observation on  $\text{NaTaO}_3$  photocatalyst particles doped with Sr cations. UV-light-induced  $\Delta$ absorbance of the  $\text{NaTaO}_3$  photocatalyst presented qualitatively different spectra when excited in a vacuum<sup>19</sup> and in liquid.<sup>13</sup> The absorption quenched in liquid was assigned to electronic states localized on the surface.

One note here is about UV-light-induced  $\Delta$ absorbance reported on P25 (Degussa), one of the most well-known commercial  $\text{TiO}_2$  photocatalysts. The asymmetric absorption band that monotonously strengthened from  $4000$  to  $1000\text{ cm}^{-1}$  has been frequently reported and assigned to excited electrons.<sup>8–10,20</sup> The reported spectra are identical with those

of TIO-7 shown in Figure 2. Because P25 contains more than 70% anatase with a minor amount of rutile and a small amount of amorphous  $\text{TiO}_2$ ,<sup>21</sup> the  $\Delta$ absorbance band upon excitation is dominated by that of anatase. A minor contribution of rutile should have appeared at  $6000\text{ cm}^{-1}$ , which is outside the wavenumber ranges considered in the earlier studies of P25.

Under steady irradiation of UV light in the methanol–water mixture, methanol oxidation and water reduction should have occurred simultaneously on the photocatalysts. Infrared absorption assignable to molecular vibration of the oxidation products was not recognized, probably because their limited concentration.

The  $\text{TiO}_2$  particles might be reduced during UV irradiation in the mixture. However, ex-situ characterization of the irradiated particles to detect reduced Ti cations by using XPS was difficult. The penetration depth of UV light used in our measurements into  $\text{TiO}_2$  particles was on the order of  $10\text{ nm}$ .<sup>22</sup> The small amount irradiated particles should be mixed with other particles when transferred for ex-situ characterization.

**3.2. UV-Light Power Dependence.** Excited electrons recombine with complementary holes in the  $\text{TiO}_2$  particles. Recombination always competes with photocatalytic reactions and hence determines the quantum yield of desired reaction products. In this section, the recombination kinetics is examined in terms of UV-light power dependence of  $\Delta$ absorbance.

TIO-6 and TIO-7 particles were placed on the prism and covered with an *n*-decane droplet. The spectrometer was then purged with  $\text{N}_2$  to provide a less-reactive liquid environment to excited photocatalysts. Electrons and holes were not transferable to anaerobic decane and thus exclusively recombined in the  $\text{TiO}_2$  particles.

Figure 3a shows  $\Delta$ absorbance spectra of TIO-7 recorded at  $7000\text{--}700\text{ cm}^{-1}$ . The power density of UV light for bandgap excitation was tuned in the range of  $22\text{--}3600\text{ W m}^{-2}$ , which corresponded to  $39\text{--}6400\text{ photons s}^{-1}\text{ nm}^{-2}$ . A power range 2 or more orders of magnitude wide was suitable to characterize the recombination kinetics. An asymmetric band peaked at  $1300\text{ cm}^{-1}$  appeared, as found for the methanol–water mixture. Bleached bands at  $1600$  and  $1500\text{--}1400\text{ cm}^{-1}$  are attributed to vibrations of water and decane. TIO-7 particles are small enough to be moist even when dried in air at room temperature. Water that remained on the particle surface induced the water-related bleached band under irradiation in decane. The strength of the electron-induced absorption was quantified with  $\Delta$ absorbance at  $1267\text{ cm}^{-1}$  and shown in Figure 3c as a function of UV light power density  $P$ .

A straight line representing  $P^{0.50}$  fitted the results (red dots) observed with  $P > 2000\text{ W m}^{-2}$ . The  $1/2$ -order power law suggests recombination of multiple electrons and holes randomly moving in each anatase particle. The rate of excitation per second is proportional to  $P$ , while the recombination rate is expressed in terms of the number of electron–hole collisions per second. The rates of excitation and recombination are balanced in the steady state:

$$P \propto \text{electron excitation rate} = \text{recombination rate} \\ = k[\text{electron}][\text{hole}] \quad (1)$$

with electron population  $[\text{electron}]$ , hole population  $[\text{hole}]$ , and a second-order rate constant  $k$ . In the absence of a redox reaction on the decane–particle interface, an equivalent number of electrons and holes are present in a particle, leading to the  $1/2$ -order power law:



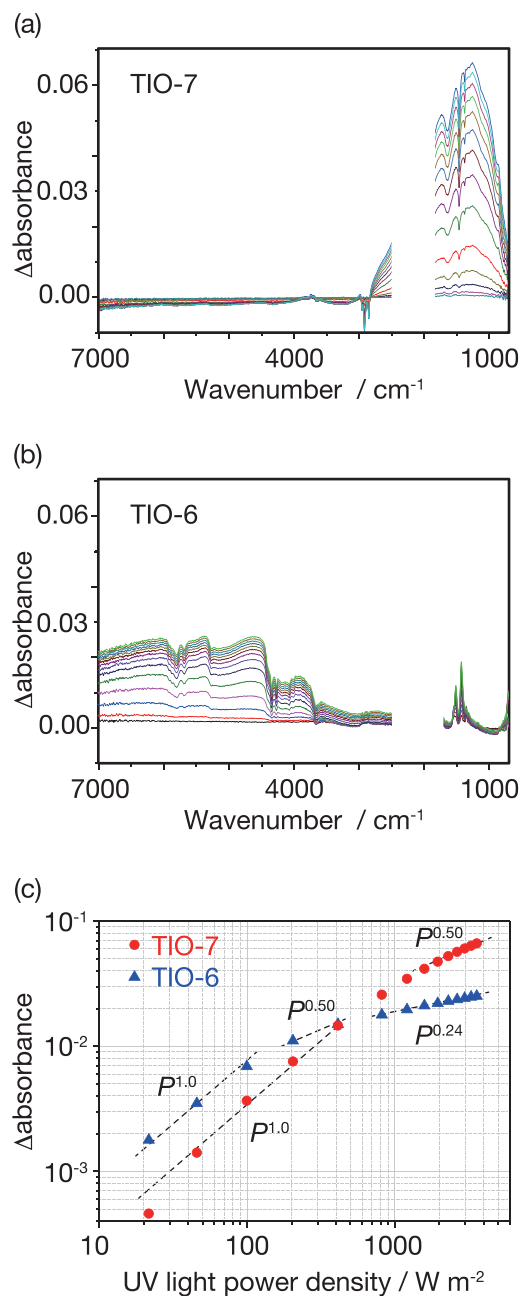


**Figure 3.** UV-light-induced  $\Delta$ absorbance spectra of (a) TIO-7 and (b) TIO-6 in anaerobic *n*-decane. UV light power density: 22, 46, 100, 200, 410, 820, 1200, 1600, 2000, 2300, 2600, 3000, 3300, and 3600 W m<sup>-2</sup>. (c) A log–log plot of  $\Delta$ absorbance on TIO-7 (red dots) and TIO-6 (blue triangles) as a function of light power density,  $P$ . Broken lines show  $P^{1.0}$ ,  $P^{0.50}$ , and  $P^{0.24}$  laws fitted to the observations.  $\Delta$ absorbance is quantified at 1267 cm<sup>-1</sup> for TIO-7 and at 6000 cm<sup>-1</sup> for TIO-6. UV light source: LED (M36SL3). Probe light source and detector: ceramic source and MCT. The spectra are shown in the wavenumber ranges of 7000–2500 and 1800–700 cm<sup>-1</sup> because IR transmittance through the prism decreased to <30% at 2500–1800 cm<sup>-1</sup>.

$$P \propto k[\text{electron}]^2 \propto \Delta\text{absorbance}^2 \quad (2)$$

As  $P$  decreased to 400 W m<sup>-2</sup>, the power-law order gradually increased to unity. The unity order claims full contribution of weak excitation, where a limited number of UV photons are absorbed in a particle. When neighboring places of UV-photon absorption are separated in space, recombination requires

collision of an electron and a hole that were created by the same photon. The electron–hole collision rate is proportional to the number of electron–hole pairs created by the same photon [electron–hole pair], leading to the first-order power law with a rate constant  $k'$ :

$$P \propto k'[\text{electron–hole pair}] \propto \Delta\text{absorbance} \quad (3)$$

The power-law order shifted to unity with  $P < 400$  W m<sup>-2</sup>. The intensity of natural solar light on the surface of Earth's atmosphere is 1.4 kW m<sup>-2</sup>.<sup>23</sup> When the fraction of UV light for bandgap excitation is 5% of the total solar irradiation, electrons and holes recombine according to eq 3 in TIO-7 particles under solar light on the ground. This indicates the dominant role of weak excitation in real TiO<sub>2</sub> photocatalysts. Because excitation and decay dynamics are often traced in TAS with highly intense light pulses, we should be careful to transfer knowledge reported in TAS to reaction kinetics on real photocatalysts. A light pulse of 10 ns in time width and 1 mJ cm<sup>-2</sup> in power density, which numbers are typical for excitation in TAS, provide a peak light power density of 1 GW m<sup>-2</sup>.

$\Delta$ absorbance spectra of TIO-6 are shown in Figure 3b. The symmetric band maximized at 6000–5000 cm<sup>-1</sup> appeared as was observed in the methanol–water mixture. The strength of the electron-induced absorption was quantified with  $\Delta$ absorbance at 6000 cm<sup>-1</sup> and is indicated with blue triangles in Figure 3c. Water overtones bleached on moist TIO-6 particles produced negative peaks at 5300–4700 cm<sup>-1</sup>. Bleaching at 5900–5600 and 4400–3900 cm<sup>-1</sup> was ascribed to overtones of decane vibrations. The fundamental tone of decane vibration produced positive peaks at 1600–1300 cm<sup>-1</sup>. The unusual behaviors, bleached overtones accompanied by enhanced fundamental tones, may be ascribed different depths of probing in the photocatalyst–decane suspension. Probing depth on the prism should be proportional to the wavelength of the probe light.

With  $P < 100$  W m<sup>-2</sup>,  $\Delta$ absorbance of TIO-6 was proportional to  $P$ , indicating pair recombination formulated in eq 3. When  $P$  was increased to 200–400 W m<sup>-2</sup>, the power-law order decreased to 1/2, suggesting random-walk recombination of multiple electrons and holes in this power density range. When power density was increased to 800–3600 W m<sup>-2</sup>, an even flatter power law,  $P^{0.24}$ , fitted the results. It is not easy to physically interpret a 0.24-order power law. We hypothesize that the power-law order decreases to zero under greater UV-light intensity. The observed  $P^{0.24}$  law indicates a transition from the 1/2-order law to the zero-order law. The zero-order law suggests the number of excited electrons saturated in a particle. When the number of electrons and holes exceeds the saturation limit, a quick recombination path may open in addition to the ordinary random-walk recombination. Another hypothesis can be proposed when the  $P^{0.24}$  law is recognized as a 1/4-order law. A redox reaction requiring four electrons to complete presents a 1/4-order law. Four-electron reduction of molecular oxygen, resident in the decane droplet or the moist surface of particles, is taken into consideration. The hypotheses for the  $P^{0.24}$  law are to be tested further.

The probing depth of 6000 cm<sup>-1</sup> light was estimated to be 0.25  $\mu$ m over the prism. Multiple layers of TIO-6 particles were present in the probed volume. If UV absorption of particles in contact with the prism was bleached under intense UV irradiation, particles deposited on the bleached particles and not yet bleached would absorb UV light penetrating through the bleached particles. Hence, bleaching of bandgap absorption is not a reason for the saturated  $\Delta$ absorbance.

## 4. DISCUSSION

### 4.1. Number of Electrons Excited in a TIO-6 Particle.

Bogomolev and Mirlin<sup>7</sup> observed near-IR absorption in rutile single crystals doped with lithium cations. The embedded Li atoms became completely ionized in the host lattice at 300 K, donating one electron per atom. They observed a symmetric spectrum with a peak at  $6600\text{ cm}^{-1}$  (Figure 3 of ref 7) and assigned the absorption to electrons donated to the host lattice. The spectrum reported in Li-doped crystals was similar to that observed in TIO-6. Here, we estimated the electron population in a TIO-6 particle by assuming that the molar absorption coefficients of electrons donated in Li-doped crystals and electrons excited in TIO-6 are the same.

With a Li concentration of  $8.6 \times 10^{16}\text{ atoms cm}^{-3}$ , which corresponds to the same number of donated electrons, the absorption coefficient was  $1\text{ cm}^{-1}$ .<sup>7</sup> Suppose that the volume probed by  $6000\text{ cm}^{-1}$  light was filled with TIO-6 particles. Because the probing depth was  $0.25\text{ }\mu\text{m}$ , TIO-6 particles with  $8.6 \times 10^{16}$  excited electrons  $\text{cm}^{-3}$  present a  $\Delta\text{absorbance}$  of  $2.5 \times 10^{-5}$ . In the results shown in Figure 3c,  $\Delta\text{absorbance}$  was 0.023 with  $P = 2000\text{ W m}^{-2}$ . Hence, the number density of excited electrons at this light power density was estimated to be  $8 \times 10^{19}\text{ electrons cm}^{-3} = 0.08\text{ electron nm}^{-3}$ .

Although it is difficult to precisely determine the probing depth as well as the fraction of the probed volume filled with particles, estimating the order of magnitude is still meaningful. The number density of excited electrons estimated in the preceding paragraph indicates that a TIO-6 particle having a spherical diameter of 15 nm steadily contained 140 electrons under UV irradiation of  $P = 2000\text{ W m}^{-2}$ . When decreasing  $P$  to  $20\text{ W m}^{-2}$ , 9 electrons are present in a particle to produce the  $\Delta\text{absorbance}$  of 0.0015 as shown in Figure 3c. A significant number of excited electrons and holes remain active in TIO-6 particles excited with LED light in decane. The estimated number of excited electrons provides an insight of rutile photocatalyst particles. Although optical absorption of electrons excited in  $\text{TiO}_2$  particles has been observed in a number of earlier studies,<sup>1,8–12,18,19,22,24,25</sup> the number of the excited electrons was difficult to be evaluated.

A spherical TIO-6 particle received  $6.5 \times 10^3\text{ photons s}^{-1}$  per particle under 365 nm light of  $P = 20\text{ W m}^{-2}$ . When received photons are fully absorbed in the particle to present 9 electrons in a steady state, the average lifetime of excited electrons defined by eq 4 should be 1 ms.

$$\text{average lifetime} = \frac{\text{steady number of excited electrons}}{\text{number of electrons excited per second}} \quad (4)$$

The 365 nm light of  $20\text{ W m}^{-2}$  simulated UV light in solar irradiation. Excited electronic states active for milliseconds were quantified as supposed in the Introduction.

**4.2. Polaronic Character of Electrons Probed by IR and Near-IR Absorption.** Here, we discuss the identity of the electrons excited in rutile and anatase particles following earlier studies.<sup>24</sup> When an electron is excited across the bandgap in rutile, the ionic lattice is deformed around the excited electron, creating a small polaron. A polaron is defined as the excess electron self-trapped in a Coulombic potential well, produced by the shifting of ions from their equilibrium positions.<sup>25</sup> When the wave function of the self-trapped electron collapses on one Ti cation, which was originally  $\text{Ti}^{4+}$ , it is recognized as a small electron polaron, as illustrated in Figure 4a.

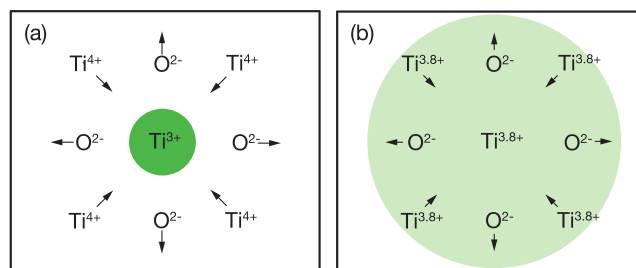


**Figure 4.** Illustration of electron polarons in  $\text{TiO}_2$ . (a) Small and (b) large polarons are illustrated in a virtual, square lattice of titanium cations and oxygen anions. An excess electron distributes in the green area. Arrows indicate displacement of cations and anions from the carrier-free positions. In (b), the excess electron shared by five cations is displayed in order to depict the definition of a large polaron and not to suggest that an electron excited in TIO-7 is shared by five cations.

The optical transition of a small polaron is energetically resonant to its hopping from the low-energy state of one cation to the high-energy state of a neighboring cation. The absorption spectrum is symmetric because of resonance with a state-to-state transition. In fact, optical absorption studies<sup>6,7,11</sup> reported a symmetric absorption peak at around  $6000\text{ cm}^{-1}$  (0.7 eV). A valence-band photoemission study<sup>26</sup> accordingly found symmetric emission bands at 1.0 eV below the Fermi level on single-crystalline rutile wafers modified by Na adatoms. The Na adatoms are supposed to produce small polarons in rutile by donating electrons. Our absorption spectra shown in Figures 2 and 3 are consistent with the reported results and indicate that bandgap-excited electrons are accommodated as small polarons in rutile particles in liquid. The steady number of electron polarons was estimated 140 per TIO-6 particle irradiated with  $P = 2000\text{ W m}^{-2}$  in Section 4.1. Because a rutile particle having a spherical diameter of 15 nm includes  $5.8 \times 10^3$  Ti cations, 0.2% of Ti cations were reduced to the 3+ state during irradiation.

In contrast to rutile, anatase is a host of large electron polarons, while the formation of small polarons in this polymorph is debated.<sup>24</sup> Figure 4b depicts the excess electron distributed over multiple Ti cations in a large polaron. When the electron is photoexcited from the ground state of the self-trapping potential well to unbound continuum states, optical absorption of an asymmetric spectrum appears.<sup>25</sup> The low-energy threshold of the absorption is determined by the energy gap between the self-trapped state and the bottom of the continuum states. The absorption coefficient decreases when the photon energy is above the threshold, generating a peak close to the threshold. This is because the initial state is confined in real space and limited in momentum. The probability of optical transition decreases with the electron momentum required in the final state, i.e., the electron energy in the final state. The required momentum is provided by phonons in the host lattice.<sup>27</sup>  $\Delta\text{absorbance}$  spectra of anatase particles reported in this study and earlier studies<sup>11,12,18</sup> accurately followed the characteristics of large-polaron photoexcitation.

Finally, the UV-light-induced  $\Delta\text{absorbance}$  spectrum of TIO-7 is compared with that of a  $\text{NaTaO}_3$  photocatalyst doped with Sr cations reported in our earlier study.<sup>13</sup> Strontium-doped  $\text{NaTaO}_3$  is one of the most efficient photocatalysts for realizing the overall water-splitting reaction.<sup>28,29</sup> The  $\Delta\text{absorbance}$  spectra of TIO-7 and Sr-doped  $\text{NaTaO}_3$  were observed in anaerobic decane by using the common set of prism assembly, spectrometer, and MCT detector. The two spectra, which are normalized at each  $\Delta\text{absorbance}$  maximum and shown in Figure

5, bear a striking resemblance: a gradual increase from 3000  $\text{cm}^{-1}$  (TIO-7) or 5000  $\text{cm}^{-1}$  (Sr-doped  $\text{NaTaO}_3$ ) with

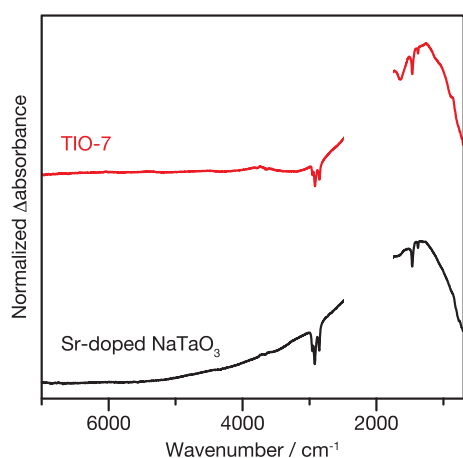


**Figure 5.** UV-light-induced  $\Delta$ absorbance spectrum of TIO-7 compared with that of a  $\text{NaTaO}_3$  photocatalyst doped with Sr cations (Sr concentration: 4 mol % relative to Ta cations). The black spectrum is adopted from Figure 1 of ref 13. The two  $\Delta$ absorbance spectra are observed in anaerobic decane. UV wavelength and power density for excitation of TIO-7: 365 nm and 3600  $\text{W m}^{-2}$ . UV wavelength and power density for excitation of Sr-doped  $\text{NaTaO}_3$ : 285 nm and 19  $\text{W m}^{-2}$ . The two spectra are normalized at each  $\Delta$ absorbance maximum and shown in the wavenumber ranges of 10000–2500 and 1800–700  $\text{cm}^{-1}$  because IR transmittance through the prism decreased to <30% at 2500–1800  $\text{cm}^{-1}$ .

absorption maxima at 1400–1300  $\text{cm}^{-1}$  and cutoff at 1000  $\text{cm}^{-1}$ . The analogous spectra suggest analogous identity of the initial and final states in the optical transition. We therefore propose here that bandgap-excited electrons created large polarons in the Sr-doped  $\text{NaTaO}_3$  photocatalyst. Because the identity of electrons excited across the bandgap of  $\text{NaTaO}_3$  is unknown, the assignment to large polarons proposed here delivers an insight of  $\text{NaTaO}_3$  photocatalysts efficient for the overall water splitting reaction.

Theoretical<sup>30–33</sup> and experimental<sup>34–37</sup> studies have emphasized the role of polarons in the control of the carrier transport rate in metal oxides. Modification of the overpotentials of surface redox reactions is also predicted with polarons.<sup>38–41</sup> Methods, results, and interpretations delivered in this study provide easy access to electron polarons in semiconductor photocatalysts excited in liquid. Light-excited hole polarons are detectable with IR absorption, as was reported on a ZnO wafer placed in vacuum and probed with a reflection setup.<sup>34</sup> ATR-based spectroscopy has not yet been applied to holes in semiconductor photocatalysts in liquid.

## 5. CONCLUSIONS

The combination of the diamond prism assembly with the FT spectrometer enabled us to trace IR and near-IR absorption spectra of electrons excited across the bandgap of  $\text{TiO}_2$  particles in liquid. Electrons excited in the rutile particles (TIO-6) formed small polarons characterized with a symmetric absorption band with a maximum at 6000  $\text{cm}^{-1}$ . Electrons in anatase particles (TIO-7) formed large polarons, producing an asymmetric absorption band that gradually increased at wavenumbers below 5000  $\text{cm}^{-1}$  and cutoff at 1000  $\text{cm}^{-1}$ . The shapes of polaron-induced spectra were insensitive to the environment (liquid or vacuum), suggesting the electron polarons accommodated in

bulk particles. The spectrum of large electron polarons in TIO-7 resembled the absorption reported for a Sr-doped  $\text{NaTaO}_3$  photocatalyst, which suggests the presence of large polarons in  $\text{NaTaO}_3$  photocatalysts.

The kinetics of electron–hole recombination was examined on UV-light power dependence of the polaron absorption in anaerobic decane. With light power density  $P$  greater than a threshold, 200  $\text{W m}^{-2}$  on TIO-6 or 2000  $\text{W m}^{-2}$  on TIO-7, the polaron absorption was enhanced with absorbance being proportional to  $P^{1/2}$ . The observed 1/2-order power law suggested recombination of multiple electrons and holes randomly moving in each particle. Upon excitation with smaller  $P$ , the power-law order increased to unity to indicate recombination of an electron and a hole that were excited by the same photon. An average polaron lifetime of 1 ms was estimated in TIO-6 particles irradiated at  $P = 20 \text{ W m}^{-2}$ . Thus, this study demonstrated the feasibility of the diamond prism combined with the FT spectrometer for characterizing and quantifying electronically excited states active for milliseconds, which should play a major role in photocatalytic reactions under solar light. Applications to a broad range of photofunctional materials hybridized with quantum dots, plasmonic nanoparticles, or 2D materials are promising.

## ■ ASSOCIATED CONTENT

### Supporting Information

The Supporting Information is available free of charge at <https://pubs.acs.org/doi/10.1021/acs.jpcb.2c07433>.

Reagents; near-IR absorption spectra of the prism assembly (Figure S1) and liquid droplets (Figure S2); X-ray diffraction patterns (Figure S3) of TIO-6 and TIO-7 photocatalyst particles; UV-light-induced absorbance change in the hole scavengers (Figure S4) (PDF)

## ■ AUTHOR INFORMATION

### Corresponding Authors

Zhebin Fu – Department of Chemistry, School of Science, Kobe University, Kobe, Hyogo 657-8501, Japan; [orcid.org/0000-0003-1017-4955](https://orcid.org/0000-0003-1017-4955); Email: [fu@harbor.kobe-u.ac.jp](mailto:fu@harbor.kobe-u.ac.jp)

Hiroshi Onishi – Department of Chemistry, School of Science, Kobe University, Kobe, Hyogo 657-8501, Japan; Research Center for Membrane and Film Technology, Kobe University, Kobe, Hyogo 657-8501, Japan; Division of Advanced Molecular Science, Institute for Molecular Science, Okazaki, Aichi 444-8585, Japan; [orcid.org/0000-0003-1873-9105](https://orcid.org/0000-0003-1873-9105); Email: [oni@kobe-u.ac.jp](mailto:oni@kobe-u.ac.jp)

Complete contact information is available at: <https://pubs.acs.org/10.1021/acs.jpcb.2c07433>

### Notes

The authors declare no competing financial interest.

## ■ ACKNOWLEDGMENTS

The authors thank Dr. Yi Hao Chew (Kobe University) for his comments on the manuscript. This study was supported by JSPS KAKENHI (Grants 18KK0161, 19H00915, and 22H00344).

## ■ REFERENCES

- (1) Iwata, K.; Takaya, T.; Hamaguchi, H.; Yamakata, A.; Ishibashi, T.; Onishi, H.; Kuroda, H. Carrier Dynamics in  $\text{TiO}_2$  and  $\text{Pt/TiO}_2$  Powders Observed by Femtosecond Time-Resolved Near-Infrared



Spectroscopy at a Spectral Region of 0.9–1.5  $\mu\text{m}$  with the Direct Absorption Method. *J. Phys. Chem. B* **2004**, *108*, 20233–20239.

(2) Paz, Y. Transient IR spectroscopy as a tool for studying photocatalytic materials. *J. Phys.: Condens. Matter* **2019**, *31*, 503004.

(3) Kranz, C.; Wächter, M. Characterizing photocatalysts for water splitting: from atoms to bulk and from slow to ultrafast processes. *Chem. Soc. Rev.* **2021**, *50*, 1407–1437.

(4) Takanabe, K. Addressing fundamental experimental aspects of photocatalysis studies. *J. Catal.* **2019**, *370*, 480–484.

(5) Kosaka, T.; Teduka, Y.; Ogura, T.; Zhou, Y.; Hisatomi, T.; Nishiyama, H.; Domen, K.; Takahashi, Y.; Onishi, H. Transient Kinetics of  $\text{O}_2$  Evolution in Photocatalytic Water-Splitting Reaction. *ACS Catal.* **2020**, *10*, 13159–13164.

(6) Cronmeyer, D. C. Electrical and Optical Properties of Rutile Single Crystals. *Phys. Rev.* **1952**, *87*, 876–886.

(7) Bogomolov, V. N.; Mirlin, D. N. Optical Absorption by Polarons in Rutile ( $\text{TiO}_2$ ) Single Crystals. *Phys. Status Solidi* **1968**, *27*, 443–453.

(8) Yamakata, A.; Ishibashi, T.; Onishi, H. Time-Resolved Infrared Absorption Spectroscopy of Photo-Generated Electrons in Platinized  $\text{TiO}_2$  Particles. *Chem. Phys. Lett.* **2001**, *333*, 271–277.

(9) Panayotov, D. A.; Yates, J. T., Jr. n-type doping of  $\text{TiO}_2$  with atomic hydrogen-observation of the production of conduction band electrons by infrared spectroscopy. *Chem. Phys. Lett.* **2007**, *436*, 204–208.

(10) Panayotov, D. A.; Burrows, S. P.; Morris, J. R. Infrared spectroscopic studies of conduction band and trapped electrons in UV-photoexcited, H-atom n-doped, and thermally reduced  $\text{TiO}_2$ . *J. Phys. Chem. C* **2012**, *116*, 4535–4544.

(11) Yamakata, A.; Vequizo, J. J. M.; Matsunaga, H. Distinctive Behavior of Photogenerated Electrons and Holes in Anatase and Rutile  $\text{TiO}_2$  Powders. *J. Phys. Chem. C* **2015**, *119*, 24538–24545.

(12) Shinoda, T.; Murakami, N. Photoacoustic Fourier Transform Near- and Mid-Infrared Spectroscopy for Measurement of Energy Levels of Electron Trapping Sites in Titanium(IV) Oxide Photocatalyst Powders. *J. Phys. Chem. C* **2019**, *123*, 12169–12175.

(13) Fu, Z.; Hirai, T.; Onishi, H. Long-Life Electrons in Metal-Doped Alkali-Metal Tantalate Photocatalysts Excited under Water. *J. Phys. Chem. C* **2021**, *125*, 26398–26405.

(14) The refractive index at 1  $\mu\text{m}$  wavelength of diamond and water was quoted from the *CRC Handbook of Chemistry and Physics*, 92nd ed.; Haynes, W. M., Lide, D. R., Eds.; CRC Press: Boca Raton, FL, 2011; Chapters 10 and 12.

(15) Yamakata, A.; Ishibashi, T.; Onishi, H. Time-Resolved Infrared Absorption Study of Nine  $\text{TiO}_2$  Photocatalysts. *Chem. Phys.* **2007**, *339*, 133–137.

(16) Ohno, T.; Haga, D.; Fujihara, K.; Kaizaki, K.; Matsumura, M. Unique Effects of Iron(III) Ions on Photocatalytic and Photoelectrochemical Properties of Titanium Dioxide. *J. Phys. Chem. B* **1997**, *101*, 6415–6419.

(17) Sayama, K.; Mukasa, K.; Abe, R.; Abe, Y.; Arakawa, H. Stoichiometric water splitting into  $\text{H}_2$  and  $\text{O}_2$  using a mixture of two different photocatalysts and an  $\text{IO}_3^-/\text{I}^-$  shuttle redox mediator under visible light irradiation. *Chem. Commun.* **2001**, 2416–2417.

(18) Savory, D. M.; McQuillan, A. J. IR spectroscopic behavior of polaronic trapped electrons in  $\text{TiO}_2$  under aqueous photocatalytic conditions. *J. Phys. Chem. C* **2014**, *118*, 13680–13692.

(19) An, L.; Onishi, H. Electron-Hole Recombination Controlled by Doping Sites in Perovskite-Structured Photocatalysts: Sr-Doped  $\text{NaTaO}_3$ . *ACS Catal.* **2015**, *5*, 3196–3206.

(20) Warren, D. S.; McQuillan, A. J. Influence of Adsorbed Water on Phonon and UV-Induced IR Absorptions of  $\text{TiO}_2$  Photocatalytic Particle Films. *J. Phys. Chem. B* **2004**, *108*, 19373–19379.

(21) Ohtani, B.; Prieto-Mahaney, O. O.; Li, D.; Abe, R. What is Degussa (Evonik) P25? Crystalline composition analysis, reconstruction from isolated pure particles and photocatalytic activity test. *J. Photochem. Photobiol. A* **2010**, *216*, 179–182.

(22) Lewis, N. S.; Rosenbluth, M. L. Theory of Semiconductor Materials. In *Photocatalysis, Fundamentals and Applications*; Serpone,

N., Pelizzetti, E., Eds.; John Wiley and Sons: New York, 1989; pp 60–62 and Figure 3.8.

(23) Kopp, G.; Lean, J. L. A new, lower value of total solar irradiance: Evidence and climate significance. *Geophys. Res. Lett.* **2011**, *38*, L01706.

(24) Franchini, C.; Reticioli, M.; Setvin, M.; Diebold, U. Polarons in materials. *Nat. Rev. Mater.* **2021**, *6*, 560–586. and references therein.

(25) Emin, D. Optical properties of large and small polarons and bipolarons. *Phys. Rev. B* **1993**, *48*, 13691–13702.

(26) Onishi, H.; Aruga, T.; Egawa, C.; Iwasawa, Y. Modification of Surface Electronic Structure on  $\text{TiO}_2(110)$  and  $\text{TiO}_2(441)$  by Na Deposition. *Surf. Sci.* **1988**, *199*, 54–66.

(27) Moser, S.; Moreschini, L.; Jácimović, J.; Barišić, O. S.; Berger, H.; Magrez, A.; Chang, Y. J.; Kim, K. S.; Bostwick, A.; Rotenberg, E.; Forró, L.; Grioni, M. Tunable Polaronic Conduction in Anatase  $\text{TiO}_2$ . *Phys. Rev. Lett.* **2013**, *110*, 196403.

(28) Iwase, A.; Kato, H.; Kudo, A. The Effect of Alkaline Earth Metal Ion Dopants on Photocatalytic Water Splitting by  $\text{NaTaO}_3$  Powder. *ChemSusChem* **2009**, *2*, 873–877.

(29) Onishi, H. Sodium Tantalate Photocatalysts Doped with Metal Cations: Why Are They Active for Water Splitting? *ChemSusChem* **2019**, *12*, 1825–1834.

(30) Deskins, N. A.; Dupuis, M. Electron transport via polaron hopping in bulk  $\text{TiO}_2$ : a density functional theory characterization. *Phys. Rev. B* **2007**, *75*, 195212.

(31) Di Valentin, C.; Selloni, A. Bulk and Surface Polarons in Photoexcited Anatase  $\text{TiO}_2$ . *J. Phys. Chem. Lett.* **2011**, *2*, 2223–2228.

(32) Davies, D. W.; Savory, C. N.; Frost, J. M.; Scanlon, D. O.; Morgan, B. J.; Walsh, A. Descriptors for electron and hole charge carriers in metal oxides. *J. Phys. Chem. Lett.* **2020**, *11*, 438–444.

(33) Uratani, H.; Nakai, H. Simulating the Coupled Structural-Electronic Dynamics of Photoexcited Lead Iodide Perovskites. *J. Phys. Chem. Lett.* **2020**, *11*, 4448–4455.

(34) Sezen, H.; Shang, H.; Bebensee, F.; Yang, C.; Buchholz, M.; Nefedov, A.; Heissler, S.; Carbogno, C.; Scheffler, M.; Rinke, P.; et al. Evidence for photogenerated intermediate hole polarons in  $\text{ZnO}$ . *Nat. Commun.* **2015**, *6*, 6901.

(35) Bandaranayake, S.; Hruska, E.; Londo, S.; Biswas, S.; Baker, L. R. Small polarons and surface defects in metal oxide photocatalysts studied using XUV reflection-absorption spectroscopy. *J. Phys. Chem. C* **2020**, *124*, 22853–22870.

(36) Shelton, J. L.; Knowles, K. E. Thermally Activated Optical Absorption into Polaronic States in Hematite. *J. Phys. Chem. Lett.* **2021**, *12*, 3343–3351.

(37) Tanner, A. J.; Thornton, G.  $\text{TiO}_2$  Polarons in the Time Domain: Implications for Photocatalysis. *J. Phys. Chem. Lett.* **2022**, *13*, 559–566.

(38) Ji, Y.; Wang, B.; Luo, Y. Location of trapped hole on rutile- $\text{TiO}_2(110)$  surface and its role in water oxidation. *J. Phys. Chem. C* **2012**, *116*, 7863–7866.

(39) Di Valentin, C. A mechanism for the hole-mediated water photooxidation on  $\text{TiO}_2(101)$  surfaces. *J. Phys.: Condens. Matter* **2016**, *28*, 074002.

(40) Gono, P.; Wiktor, J.; Ambrosio, F.; Pasquarello, A. Surface Polarons Reducing Overpotentials in the Oxygen Evolution Reaction. *ACS Catal.* **2018**, *8*, 5847–5851.

(41) Rajan, A. G.; Martinez, J. M. P.; Carter, E. A. Why do we use the materials and operating conditions we use for heterogeneous (photo)electrochemical water splitting. *ACS Catal.* **2020**, *10*, 11177–11234.